Advanced Powder Technology 28 (2017) 2503–2513

Contents lists available at ScienceDirect

Advanced Powder Technology

journal homepage: www.elsevier.com/locate/apt

Original Research Paper

Powder reduction kinetics of dicalcium ferrite, calcium ferrite, and hematite: Measurement and modeling

Chengyi Ding [a], Xuewei Lv [a,b,*], Senwei Xuan [a], Xueming Lv [a], Gang Li [a], Kai Tang [a]

[a] School of Materials Science and Engineering, Chongqing University, China
[b] The State Key Laboratory of Mechanical Transmissions, Chongqing University, China

ARTICLE INFO

Article history:
Received 15 April 2017
Received in revised form 16 June 2017
Accepted 29 June 2017
Available online 12 July 2017

Keywords:
Powdered reduction
Dicalcium ferrite
Calcium ferrite
Hematite
Avrami-Erofeev equation

ABSTRACT

Shrinking core model is widely applied to describe the reduction of iron ore pellets, but limited to the illustration on powder sample. The reduction of powder materials is commonly observed in blast furnace production but has been rarely investigated. In this study, thermal kinetics analysis was conducted to describe the powder reduction of dicalcium ferrite ($2CaO{\cdot}Fe_2O_3$, C_2F), calcium ferrite ($CaO{\cdot}Fe_2O_3$, CF), and hematite (Fe_2O_3, H), with particle sizes below 70 μm. Isothermal reduction experiments were performed through thermogravimetry analysis under CO atmosphere. The reduction degrees and reaction rate constants increased in the order of C_2F, CF, and H at 1123, 1173, and 1223 K. The reduction rate analysis illustrated that the reduction of C_2F, CF, and H appeared as one-, two-, and three-stage reactions, respectively. Moreover, the reduction of C_2F and CF proceeded as the 2D reaction mechanism described by Avrami–Erofeev (A-E) equation. The reduction of H was initially controlled by 2D, followed by the 3D A-E kinetics equation. Phase with superior reducibility could be reduced by CO in more dimensions of sample layers. The reduction degrees and rate change expressed by A-E equations were verified to be in accordance with the experimental data. A new kinetics model was proposed to elucidate the reduction of C_2F, CF, and H in ultrafine powder compared with that in pellets. The reduction process in the powdered samples comprised independent reduction stages caused by uniform CO diffusion in powdered particles.

1. Introduction

Studies have investigated shrinking core model to describe the reduction of iron ore pellets [1–5]. Wen [6] used the shrinking core system in the reaction models of non-catalytic heterogeneous solid–fluid to determine the relationship between reaction degree and time in different stages. The model is only suitable to the reaction of non-porous solids at the interface between the external and inner unreacted cores. In large pellets with size of 1–100 mm, catalytic active substances are initially formed on the external surface of pellets without changing the reaction rate; as the substances reach the critical concentration, the reaction interface can then be generated. The reaction interface is parallel to the external surface and advances into the interior of the solid as the reaction proceeds [7]. However, in small particles with size of 1–100 μm, gas diffusion progresses easily from the outer to inner surface of the samples to reach the solid–gas reaction interface. Thus, the solid reactant receives uniform concentration of the reduction agent, the situation is different from reduction behavior of iron oxides reduced in pellet sample. The current particles in metallurgical industry mainly concentrate on pellet size (1–100 mm) and previous studies on reduction process also focused on this range of size, metallurgical study will be pushed to nanometallurgy (1–100 nm) in the future. Nanoparticles applications were fully investigated by various studies [8,9]. As the transition from traditional metallurgy to nanometallurgy, reduction on powder (1–100 μm) applications need more explorations in terms of kinetics performance, which was shown in Fig. 1. Besides, in the non-blast furnace process, for example, the FINEX® method, is used in fluidized bed for reducing iron ore [10]. The size of iron ore powder is also within 1–100 μm. This experiment can also enrich the study of fluidized reduction kinetics.

Sinters and lump ores are prepared with proper size composition to meet the required permeability of material bed for blast furnace production. Although large amounts of powdered materials are charged into a blast furnace, the reduction behavior in these materials has been less investigated compared with that in iron ore pellets. Dicalcium ferrite ($2CaO{\cdot}Fe_2O_3$, C_2F), calcium ferrite ($CaO{\cdot}Fe_2O_3$, CF), and hematite (Fe_2O_3, H) are main reduced phases

* Corresponding author at: School of Materials Science and Engineering, Chongqing University, China
E-mail address: lvxuewei@cqu.edu.cn (X. Lv).

http://dx.doi.org/10.1016/j.apt.2017.06.026
0921-8831/

Nomenclature

α	reduction degree
m_t% and m_0%	the mass percentages of removed oxygen at fixed time t and the theoretically value from iron oxide, %
dα/dt	reduction rate, min^{-1}
$k(T)$	rate constant, min^{-1}
E	apparent activation energy, kJ/mol
A	pre–exponent, min^{-1}
R	gas constant, 8.314 J(mol K)$^{-1}$
$f(\alpha)$ and $F(\alpha)$	model function and its integration
$y(\alpha)$	a defined non–dimensional parameter
I	reduction rate, mg/(min cm^2)

in fluxed sinters and lumps, the present study aims to describe the kinetics of C_2F, CF, and H as powdered samples. Reduction performance of C_2F, CF, and H in a blast furnace was expressed in Fig. 2. Mckewan [11] proposed a liner rate law of reduction kinetics for iron oxides. Bogdandy [12] reported the kinetics of gaseous reduction of iron oxides by analysis of thermodynamic stability and chemical as well as physical characteristics of original, intermediate and product phases. The kinetics of calcium ferrites was relatively complicated caused by multi-stage reduction route. Even all the previous kinetics studies focused on the iron oxides in the pellet. The kinetics parameters such as activation energy and model functions of CF and H reduction were measured by Ding [13] whereas the reduction model was not verified by fully research. A new kinetics model was proposed to elucidate the powdered reduction phenomenon in this study. The reduction of iron oxides in powdered materials widely exists in various industries, particularly in ironmaking production. Results will provide a research basis for the development of powder reduction field.

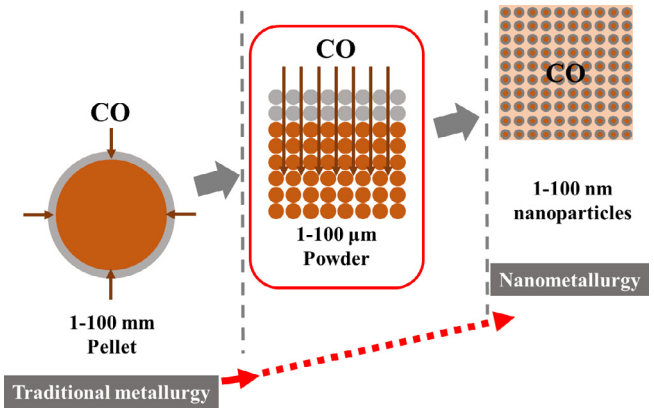

Fig. 1. Reduction on powder application is transition from traditional metallurgy to nanometallurgy.

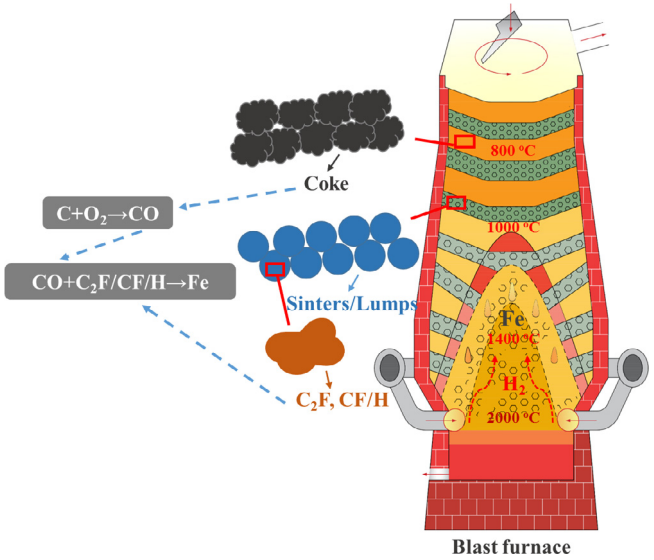

Fig. 2. Reduction performance of C_2F, CF, and H in a blast furnace.

2. Experimental

2.1. Material preparation

Samples 1, 2, and 3 were prepared from $CaCO_3$ (≥99.99%, <100 μm) and Fe_2O_3 (α-Fe_2O_3, ≥99.99%, <100 μm) with 2:1, 1:1, and 0:1 mole ratios, respectively. Powdered raw materials were uniformly mixed and pressed into cylindrical samples. The samples were roasted in a furnace with $MoSi_2$ as heating element at 1173 K (900 °C) for 1 h to completely decompose $CaCO_3$ to CaO. The temperature was increased to 1473 K (1200 °C) for 20 h to allow the complete formation of C_2F and CF. The entire process was performed in air atmosphere. The final roasted samples were ground into powder for thermogravimetry (TG) analysis.

X-ray diffraction (XRD) (Model D/max2500/PC (Cu Kα)) analysis was conducted to determine the phase composition of the samples. Scanning was performed at an angular range of 10–90°, with a scan rate of 4°/min. The XRD patterns of samples 1, 2, and 3 and the standard patterns of C_2F, CF, and H are shown in Fig. 3. The results indicate that samples 1, 2, and 3 mainly comprise C_2F, CF, and H, respectively.

The micrographs obtained by scanning electron microscope (SEM, Model TESCAN VEGA 3 LMH) and particles sizes obtained through laser particle test (Model MS2000 Malven Instrumentation) of the powdered C_2F, CF, and H samples were shown in Fig. 4. The particle sizes of the three samples are lower than 70 μm.

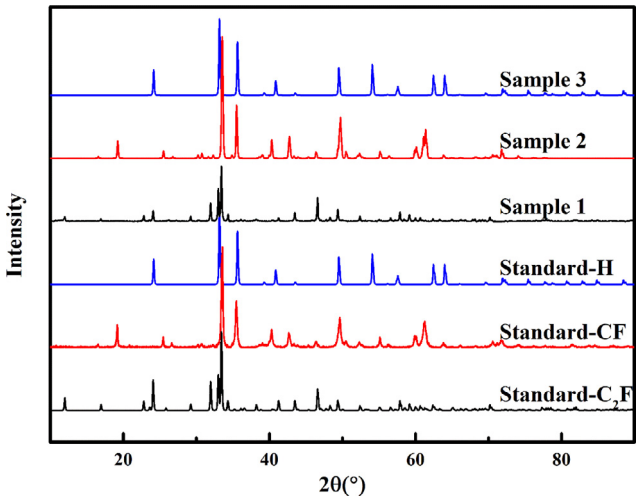

Fig. 3. XRD patterns of samples and standard patterns of C_2F, CF, and H.